

# Observations of microglitches in HartRAO radio pulsars

A. E. Chukwude<sup>1,2\*</sup>, and J. O. Urama<sup>1</sup>

<sup>1</sup>*Department of Physics & Astronomy, University of Nigeria, Nsukka, Enugu State, Nigeria*

<sup>2</sup>*Federal University of Petroleum Resources (FUPRE), PMB 1221 Effurun, Delta State, Nigeria*

30 October 2018

## ABSTRACT

A detailed observation of microglitch phenomenon in relatively slow radio pulsars is presented. Our analyses for these small amplitude jumps in pulse rotation frequency ( $\nu$ ) and/or spin down rate ( $\dot{\nu}$ ) combine the traditional manual detection method (which hinges on careful visual inspections of the residuals of pulse phase residuals) and a new, and perhaps more objective, automated search technique (which exploits the power of the computer, rather than the eyes, for resolving discrete events in pulsar spin parameters). The results of the analyses of a sample of 26 radio pulsars reveal that: (i) only 20 pulsars exhibit significant fluctuations in their arrival times to be considered suitable for meaningful microglitch analyses; (ii) a phenomenal 299 microglitch events were identified in  $\nu$  and/or  $\dot{\nu}$ : 266 of these events were found to be simultaneously significant in  $\nu$  and  $\dot{\nu}$ , while 19 and 14 were noticeable only in  $\nu$  and  $\dot{\nu}$ , respectively; (iii) irrespective of sign, the microglitches have fractional sizes which cover about 3 orders of magnitude in  $\nu$  and  $\dot{\nu}$  ( $10^{-11} < |\Delta\nu/\nu| < 2.0 \times 10^{-8}$  and  $5.0 \times 10^{-5} < |\Delta\dot{\nu}/\dot{\nu}| < 2.0 \times 10^{-2}$ ) with median values as  $0.78 \times 10^{-9}$  and  $0.36 \times 10^{-3}$ , respectively.

**Key words:** methods: data analysis – stars: neutron – pulsars: general

## 1 INTRODUCTION

Discrete discontinuities in the rotation of pulsars are broadly of two sorts: macroglitches and microglitches (e.g. Cordes, Downs & Krause-Polstorff 1988). Macroglitches (conventionally known as glitches) are characterised by a sudden increase in pulsar rotation frequency,  $\nu$ , usually accompanied by an increase in magnitude of the spin-down rate,  $\dot{\nu}$ , (e.g. Urama 2002; Wang et al. 2001; Lyne et al. 1996; Flanagan 1990; Lyne 1987; Lyne & Pritchard 1987). Macroglitches are arguably the more spectacular events, characterised by fractional changes in pulsar spin frequency ( $\Delta\nu/\nu$ ) and spin-down rate ( $\Delta\dot{\nu}/\dot{\nu}$ ) in the range of  $\sim 10^{-8} - 10^{-6}$  and  $10^{-4} - 10^{-1}$ , respectively, (Lyne, Shemar & Smith 2000; Shemar & Lyne 1996). To date, about 280 macroglitches have been reported in about 100, mostly young, pulsars (Melatos, Peralta & Wyithe 2008 and references therein). Macroglitches have been extensively studied and are now firmly associated with some unique features. The jumps in the rotation frequency ( $\Delta\nu$ ) and the spin-down rate ( $\Delta\dot{\nu}$ ) have a definite signature,  $(\Delta\nu, \Delta\dot{\nu}) = (+, -)$ , corresponding to increases in the pulsar spin rates and magnitude of the spin-down rates (Melatos et al. 2008 and references therein). It is worthy of note that positive  $\Delta\dot{\nu}$  have been reported in a few macroglitches (with  $\Delta\nu/\nu > 10^{-7}$ : see, for example, Middleditch et al. 2006;

Urama & Okeke 1999 and references therein). However, we should also mention that the error estimates in the measured values of  $\Delta\dot{\nu}/\dot{\nu}$  in all these cases are, uncomfortably, too large. For most well observed macroglitches, the jumps in the rotation frequency are accompanied by periods of relaxation towards the unperturbed pre-glitch values, which vary on a wide range of timescales (Lyne et al. 1996; Flanagan 1995, 1990; Cordes et al. 1988; Lyne 1987; Lyne & Pritchard 1987). Macroglitches are now widely believed to originate from some form of dynamical change within neutron star interior, such as a sudden and irregular transfer of angular momentum from the more rapidly rotating inner superfluid components to the slowly spinning crust (Ruderman, Zhu & Chen 1998; Alpar et al. 1996, 1984)

On the other hand, microglitches constitute a class of small amplitude, but resolvable jumps in both, or either of the pulsar rotation frequency and its first time derivative. Unlike the spectacular macroglitch events, the study of microglitches have received a far less attention in the last three decades of pulsar timing observations. As a result, very little is known about this class of rotational discontinuities (Chukwude 2002; Cordes et al. 1988). To date, only about 90 microglitches have been reported in  $\sim 20$  radio pulsars (Cordes & Downs 1985, hereafter CD85; Cordes et al. 1988; D’Alessandro et al. 1995, hereafter DA95). The amplitudes of the jumps vary over a wide range, but are generally believed to be within  $\Delta\nu/\nu < 10^{-10}$  and  $\Delta\dot{\nu}/\dot{\nu} < 10^{-3}$ .

\* E-mail: aus\_chukwude@yahoo.com

However, unlike macroglitches, where the jumps are associated with a definite signature, microglitches have all possible combination of signs and are extraordinarily difficult to understand in the framework of all known macroglitch theories (D’Alessandro 1997; Cordes et al. 1988; CD85).

Previous observations of microglitches in radio pulsars have relied solely on visual inspection of carefully calculated residuals of pulse rotation frequency and its first time derivative ( $\Delta\nu$  and  $\Delta\dot{\nu}$ , respectively). However, observational constraints have permitted only indirect calculations of  $\Delta\nu$  and  $\Delta\dot{\nu}$  via successive numerical differentiation of phase residuals obtained from 2nd-order model fits to barycentric times of pulse arrival (DA95 Cordes et al. 1988; CD85). In principle, scatters in the differentiated phase residuals that are significantly in excess of measurement uncertainties are attributed to discrete rotational discontinuities. The effectiveness of this technique for microglitch observation has, hitherto, been plagued with sparsely sampled timing data. This results in a paucity of data, which introduces significant ambiguities in both the epoch and amplitude of candidate events. For instance, the process of numerically differentiating pulse phase residuals could require data segments with widely varying lengths. Hence, candidate microglitch events whose epochs are located deep within the segments could easily be averaged out during the process, thereby reducing the overall sensitivity of the technique for microglitch observation.

A more comprehensive observational description of the phenomenon of microglitches has, however, become an indispensable part of the current quest for improved statistics of radio pulsar microglitches. This is particularly important for the much sought-after better insight into the incidence and other features of these small amplitude discontinuities in pulsar rotation. Specifically, such a description is required in order to ascertain the applicability of the various models involving the neutron star interior and/or magnetospheric torque fluctuations (e.g. Glampedakis & Andersson 2009; Melatos & Warszawski 2009; Warszawski & Melatos 2008; Melatos & Peralta 2007; Peralta et al. 2006; Link, Epstein & Baym 1993; Alpar et al. 1984; Cordes & Greenstein 1981; Arons 1981). Some potential benefits of this include a better understanding of the possible origin of microglitches and, perhaps, the relationship, if any, between macroglitches and microglitches.

In this paper, we present an in-depth observation of the phenomenon of microglitches in a sample of 26 radio pulsars. Our data, which span about 16 years for each object, are characterised by much improved sampling intervals of  $\sim 0.05$  to 40 d. The short observation intervals and the resultant high data density allowed us to introduce alternative and, perhaps, more objective methods of resolving small amplitude discrete rotational discontinuities in radio pulsars. **In a forthcoming paper, we will compare the microglitching rates and size distributions with the glitch results recently published by Melatos et al. (2008).**

## 2 OBSERVATIONS

Regular timing observations of all objects in the current sample of 26 radio pulsars commenced at Hartebeesthoek

Radio Astronomy Observatory between 1984 January and 1987 May and are still ongoing. However, only the timing data accumulated up to 2002 October are reported in this paper. HartRAO regular pulsar timing observation was, however, interrupted between 1999 June and 2000 August due to a major hardware upgrade. Only the pulsars B0833–45 and B1641–45, on real time glitch monitoring program, were scheduled during this period. The two pulsars are, nonetheless, excluded from current analysis. In HartRAO, pulse times of arrival (TOAs) were measured regularly at intervals  $\sim 1 - 14$  days using the observatory 26-m parabolic radio telescope. Pulses from radio pulsars were recorded by a single 10 MHz bandwidth receiver centred near 13 or 18 cm and no pre-detection dedispersion hardware was implemented during the period under consideration.

For each pulsar, detected pulses are smoothed with an appropriate filter-time constant, and folded over  $N_p$  consecutive rotation periods to beat down the background noise.  $N_p$  is different for different pulsars, but it generally varies between 500 and 5000 for the current sample. This corresponds to an integration time in the range of  $\sim 48$  s – 32 mins. An integration was usually started at a particular second by synchronization to the station clock, which is derived from a hydrogen maser and is referenced to the Universal Coordinated Time (UTC) via the Global Position satellite (GPS). On average, three such on-line integrations were made for each pulsar during a typical observing session. Details of data acquisition and reduction at HartRAO have been described elsewhere (Flanagan 1995).

## 3 TIMING ANALYSIS AND RESULTS

The resulting topocentric arrival times were transformed to infinite observing frequency at the Solar System Barycentre (SSB) using the Jet Propulsion Laboratory DE200 solar system ephemeris (Standish 1982) and TEMPO2 software package (Hobbs, Edwards & Manchester 2006). Subsequent modelling of the barycentric times of pulse arrival (hereafter referred to as BTOAs) and further analyses were accomplished with the HartRAO in-house pulsar timing analysis software (CPHAS), which is based on the standard pulsar timing technique (e.g. Manchester & Taylor 1977) and is well described in Flanagan (1995). To account for the pulsar deterministic spindown, the BTOAs were modelled with a simple Taylor series of the form (e.g. Lorimer & Kramer 2005)

$$\phi(t) = \phi_0 + \nu(t - t_0) + \frac{1}{2}\dot{\nu}(t - t_0)^2, \quad (1)$$

where  $\phi_0$  is the phase at an arbitrary time  $t_0$ ,  $\nu$  and  $\dot{\nu}$  are, respectively, the rotation frequency and its first time derivative. Equation (1) presumes that pulsar deterministic spindown follows a simple power-law relation of the form  $\dot{\nu} = K\nu^n$ : where  $K$  is a positive constant which depends on neutron star magnetic moment and moment of inertia and  $n$  is the torque braking index. For the simplest standard model, in which the torque braking processes are largely due to vacuum magnetodipole radiation at the pulsar rotation frequency (e.g. Goldreich & Julian 1969; Pacini 1968)  $n = 3$ . The difference between the observed BTOAs and the predictions of the best-fit model for pulsar rotation (the phase or,

more appropriately, the time residuals) are shown in Fig. 1 for a selection of six HartRAO pulsars. The observed phase residuals of six pulsars (B0450–18, B1133+16, B1426–66, B1451–68, B1933+16 and B2045–16) are dominated by intrinsic scatters of unusual large amplitudes. **The intrinsic scatter refers to a combination of flux noise and some other additional noise: which are largely due to effects such as pulse-to-pulse phase jitter, which is intrinsic to the pulsar, and interstellar scintillation, which causes fluctuations in the observed pulse strength within the integration time and bandwidth (Cordes & Downs 1985). Scatters in BTOA residuals dominated by these noise processes more or less have white noise statistics, irrespective of their amplitudes (e.g. Chukwude 2002).** The sizes of the BTOAs scatters suggest that they could have completely swallowed up any genuine, smaller amplitude timing noise activity inherent in these objects. For these peculiar pulsars, the rms timing noise ( $\sigma_{\text{TN}} = \sqrt{\sigma_{\text{R}}^2 - \sigma_{\text{W}}^2}$ : where  $\sigma_{\text{R}}$  is the root-mean-squares phase residuals from 2nd-order polynomial (i.e. a model  $[\nu, \dot{\nu}]$ ) fit to the entire data span and  $\sigma_{\text{W}}$  is the rms white noise) is less than 5 mP. Estimates of  $\sigma_{\text{W}}$  were obtained using pairs of BTOA residual data, from 2nd-order models, whose separations do not exceed 1 day (see, e.g. Chukwude 2002). The signal-to-noise ratio ( $\text{SNR} = \sigma_{\text{R}}/\sigma_{\text{R}}$ ) of these objects are typically less than 3 and they are excluded from further microglitch analysis in this paper. For the remainder of 20 pulsars, the observed SNR lie between  $\sim 8$  and 700, suggesting a wide dispersion in the level of the observed timing activity. The phase residuals of some of the objects (e.g. B0740–28, B1323–62, B1356–60 and B1749–28) are characterised by series of sudden slope changes. Such discontinuous rotational behaviour have been widely attributed to enhanced activity of small-amplitude discrete rotational jumps (Chukwude 2002; D’Alessandro & McCulloch 1997; CD85).

### 3.1 BTOA Error Assignment

Assignment of correct errors to the pulse times of arrival data is crucial for a meaningful microglitch analysis. Such analysis usually involves a careful calculation of numerical values of small amplitude jumps in pulsar spin parameters, the associated formal errors and the determination of the significance of the jump parameters relative to the formal errors. Therefore, an accurate BTOA error assignment improves both the sensitivity of the technique and the reliability of the results. In order words, under- or over-estimation of the errors assigned to BTOAs would seriously affect the results of any glitch analysis, especially the microglitches. Correct assignment of BTOA errors is particularly important for the newly introduced automated microglitch detection technique. This technique employs the goodness of fit parameter, which relies heavily on correctly weighted least-square fits, as a tracer of microglitch events.

Unfortunately, the formal BTOA errors returned by the HartRAO in-house routines used to extract arrival times from observations are known to be grossly underestimated (Flanagan 1995). Consequently, realistic BTOA errors are obtained from the real scatter in the BTOA data (Flanagan 1995). Short segments of data, spanning between  $\sim 50$  and 200 days, are modelled with 2nd-order polynomial plus

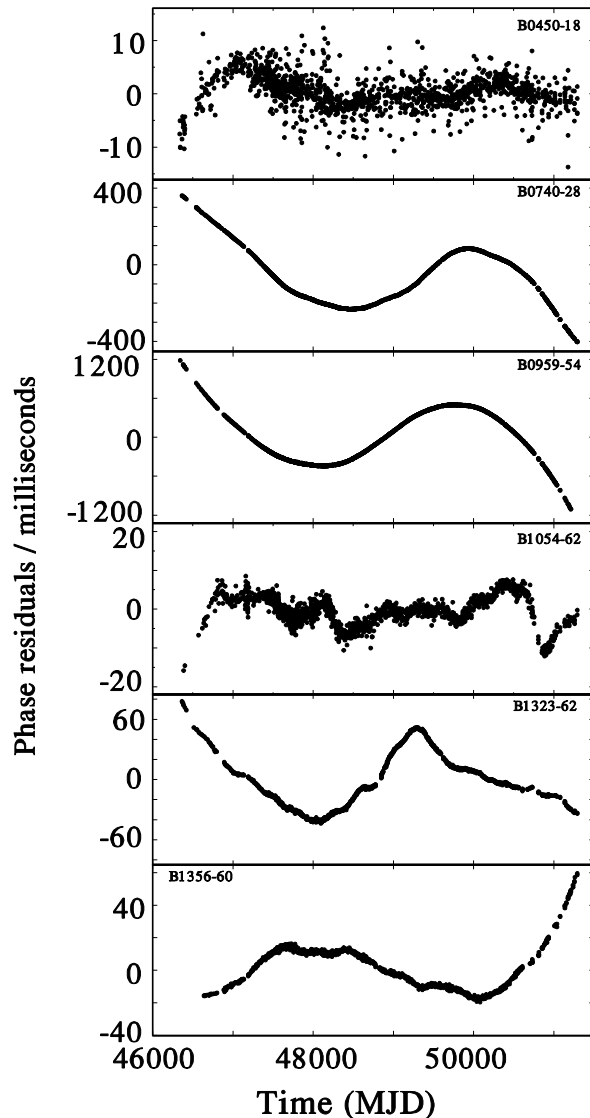


**Figure 1.** The phase residuals, defined in the sense of model-predicted minus observed BTOAs, for a selection of 6 HartRAO radio pulsars over the interval between 1984 and 1999. The pulsar B0450–18 typifies objects whose BTOA residuals over the  $\sim 13$ -yr period are dominated by large amplitude scatter, which have predominantly white noise statistics. Meaningful microglitch analyses were, generally, not possible for this category of pulsars using current techniques.

a dispersion measure (DM) term. The length of the segments, which depended on both the timing activity level and the density of BTOAs, is such that the resulting phase residuals are statistically equal to zero. Hence, the segment lengths are expected to be shorter for pulsars with enhanced microglitch activity or near epochs of macroglitches to compensate for the expected additional scatter. The residuals are manually examined for possible outliers, which could bias the error estimates. Finally, BTOA errors are calculated from the real scatter in the phase residuals. Our estimator (following Flanagan 1995) is the two-sample variance calculated over successive blocks of length  $\Delta T$ : where  $\Delta T \sim 5 - 10$  days, depending on the data sampling rates. The error assigned to each BTOA is the rms of the two-sample variance

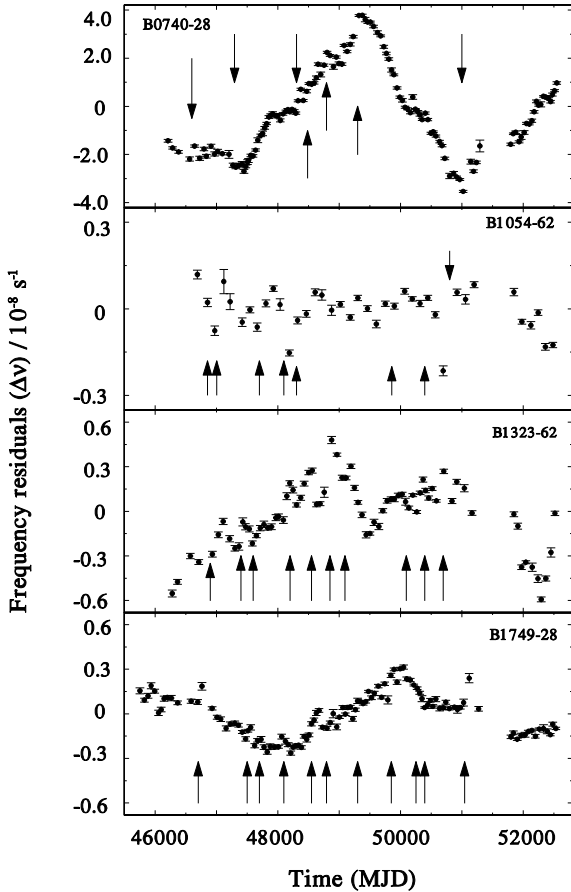


**Figure 2.** Time evolution of the frequency residuals ( $\Delta\nu(t)$ ), calculated as described in the text, for a selection of 4 HartRAO pulsars over the period between 1984 and 2001. Arrows indicate the points where scatters in  $\Delta\nu$  are significantly ( $> 2\sigma$ ) larger than the measurement uncertainties, suggestive of the occurrence of real jump in the pulsar rotation. Error bars are  $1\text{-}\sigma$  formal standard errors.

of the block within which it falls. Although this method, unfortunately, results in BTOA data errors not being strictly independent, this problem is somewhat alleviated since our model fits involve data lengths  $T$  (where  $T \gg \Delta T$ ). The 13 and 18 cm observations were separately analysed, since the amplitudes of the observed scatter are different at the two frequencies. BTOA errors calculated using this method are found to be larger than those returned by the fitting routine, on average, by factors of  $\sim 2$  and 4 for the 18 and 13 cm data, respectively. It has been shown (Chukwude 2007; Urama 2002; Flanagan 1995) that BTOA uncertainties obtained in this manner represent more realistic estimates.

### 3.2 Manual search for microglitches

As usual, the manual technique for microglitch detection relies largely on visual inspections of plots of carefully calculated residuals of pulsar spin frequency ( $\Delta\nu$ ) and/or its first derivative ( $\Delta\dot{\nu}$ ) for scatters significantly in excess of the measurement uncertainties. The frequency and spin-down rate residuals can be calculated either directly, using coefficients of local fits of 2nd-order polynomial model to short spans of BTOAs (Flanagan 1995; Cordes et al. 1988), or in-

directly, by numerically differentiating phase residuals (e.g. DA95; CD85). The apparent high quality of the current data (high density of BTOAs) allowed us to implement the former method, which promises to be more sensitive to small discrete discontinuities.

For each of the 20 pulsars, a time series of the pulsar rotation frequency ( $\nu(t)$ ) were calculated by performing weighted least-square fits of a 2nd-order polynomial to short independent blocks of BTOAs. The block lengths were determined by the data sampling rates, the intrinsic scatter in the BTOAs and our desire to keep the formal errors in  $\nu$  to  $\sim 1$  part in  $10^9$ . These constraints resulted in segment lengths in the range of 35 – 120 days. The frequency residuals ( $\Delta\nu(t)$ ) were calculated as the differences between the raw data ( $\nu(t)$ : obtained from local fits to independent short segments of BTOAs) and a model  $[\nu, \dot{\nu}]$  fitted to the entire data span length (with epoch near the midpoint of the data). The frequency residuals of 4, out of the 20, pulsars used in current analysis are shown in Fig. 2. The  $\Delta\nu - t$  plots were carefully inspected for evidence for possible discontinuous rotation, usually depicted by scatters whose amplitudes are significantly ( $> 1\text{-}\sigma$ ) larger than the error bars. Generally, such large rotational discontinuities were interpreted as signatures of microglitch events and the unrefined epochs of the events were read directly from the horizontal axis of the graph. The unrefined epochs of some of the candidate microglitch events are marked with arrows in Fig. 2.

Once a candidate event had been identified in this manner, short data segments spanning  $\sim 200\text{--}400\text{-d}$ , and bracketing the candidate microglitch event were modelled with a 2nd-order polynomial. The resulting phase residuals were carefully re-examined for evidence for a discontinuous rotation, easily seen as a sudden slope change in the observed residuals. Such a sudden slope change is attributed to a microglitch event and the epoch is now obtained directly from the phase residual plots. Fig. 3 shows typical examples of the phase residuals from short segments known to harbour one or more candidate events, first identified with the  $\Delta\nu$  plots. **Basically, possible candidate events are simply depicted by sudden slope changes in the observed phase residuals** In principle, this approach, generally, results in improved epochs of candidates events, with epoch uncertainties reduced to observation intervals.

The relevant jump parameters (the epoch, the sizes of the jumps in  $\nu$  and  $\dot{\nu}$ :  $\Delta\nu$  and  $\Delta\dot{\nu}$ , respectively) were estimated by separately modelling the BTOA data extending between 200 and 400 d on both sides of an identified event with equation (1). This method resulted in two sets of ephemerides for each event.  $\Delta\nu$  and  $\Delta\dot{\nu}$  were estimated, respectively, from  $\Delta\nu = \nu_{\text{post}} - \nu_{\text{pre}}$  and  $\Delta\dot{\nu} = \dot{\nu}_{\text{post}} - \dot{\nu}_{\text{pre}}$  (Chukwude 2002). The parameters  $\nu_{\text{pre}}$  and  $\dot{\nu}_{\text{pre}}$  refer to the pre-event values extrapolated to the event epoch, while  $\nu_{\text{post}}$  and  $\dot{\nu}_{\text{post}}$  are the corresponding post-event values, also extrapolated to the event epoch. Current method identified 124 candidate discrete jumps in  $\nu$  and/or  $\dot{\nu}$ : about 80 were noticeable simultaneously in  $\nu$  and  $\dot{\nu}$  while 25 and 19 were identified in only  $\nu$  and  $\dot{\nu}$ , respectively.

### 3.3 Automated search for microglitches

The current automated (or at least semi-automated) method for detecting microglitches was developed and applied in

analysis of Vela pulsar data (Flanagan 1995). The technique employs a statistic, the “goodness of fit” parameter ( $Q$ ), to determine when the model fit to BTOAs suddenly becomes too bad, probably, due to discrete rotational discontinuity. In HartRAO, the least-squares fitting routine employed in pulsar timing analysis uses a version of CURFIT of Bevington (1969), as modified by Flanagan (1995). Some of the outputs of the modified CURFIT include the chi-square ( $\chi^2$ ) and the reduced chi-square ( $\chi_R^2 = \chi^2/dof$ , where  $dof$  is the number of degrees of freedom of the fit). The goodness of fit parameter  $Q$  is estimated by calculating the probability of obtaining the measured value of  $\chi_R^2$  from the data, assuming that the fitted model is the correct one. Following Flanagan (1995),  $Q = Q(dof/2, \chi^2/2)$ , where  $Q = Q(dof/2, \chi^2/2)$  is the incomplete gamma function. However, the calculation of meaningful  $Q$  values is strongly dependent on the availability of sensible estimates of the BTOA errors employed in the weighted least-squares fits. As a result, extra efforts are required in order to estimate realistic pulse times of arrival uncertainties provided to the fitting routine. This is extremely important in order to minimise the sensitivity of  $Q$  values to seeming outlier BTOA data.

In this method, weighted least-square fits are performed. About 50–100-d block of BTOAs was modelled with equation (1) plus a DM term. The block length was subsequently incremented in steps of 7 d, corresponding roughly to the mean observation interval, until  $Q$  value suddenly dropped below 0.1. A broad-brush approach is to interpret such a low  $Q$  value as suggesting a poor description of the data by the model, due to a small discrete jump in the pulsar rotation. The resulting ephemerides were written to a file. The procedure was repeated, now starting from the epoch of this presumed event, until the end of the data set was reached (hereafter referred to as forward pass). The entire process – identification of candidate events, writing of the ephemerides to a file and restarting the model-fits – is automated. Hence, once the parameters are properly set up, a complete pass through the data was achieved, with minimum manual intervention. To ensure that very small amplitude events were not averaged out, the  $\sim 50$ -d start block was staggered by  $\sim 20$  d, at a time, and the whole process was repeated. **The staggered fits improved the sensitivity of the automated search technique, as it identified a few more microglitch events which were completely averaged out in the relatively long start blocks.** Finally, the process was repeated starting from the end of a data set, and going backwards until the start of the data is reached (hereafter referred to as backward pass).

The results of these procedures were sets of ephemeris files containing ephemerides extending on both sides of the candidate microglitch events. The epoch of an event was taken as the average of the two arrival times bracketing the event and the jump parameters,  $\Delta\nu = \nu_{\text{post}} - \nu_{\text{pre}}$  and  $\Delta\dot{\nu} = \dot{\nu}_{\text{post}} - \dot{\nu}_{\text{pre}}$ , were calculated as the difference between consecutive ephemerides after extrapolating to the event epoch. In most cases, real discrete discontinuities identified in forward pass were also detected in the backward pass with nearly coincident epochs and jump parameters of opposite signs, but of almost equal magnitudes. The automated technique identified 330 candidate discrete jumps simultaneously in  $\nu$  and  $\dot{\nu}$ . Additional 80 and 130 events were resolved separately in  $\nu$  and  $\dot{\nu}$ , respectively. As expected, the automated

technique equally identified all the manually observed candidate events, as evidenced by the nearly coincident epochs and jump parameters of similar size and signs. However, it was observed that the parameters of these microglitches were generally better resolved by the manual technique. **Currently, we are not aware of any serious systematic bias in the techniques implemented in the current analysis. A possible bias in the automated search method could have resulted from BTOA data points with grossly underestimated errors. However, the resulting spurious events, which would be characterised by significantly different epochs in the forward and backward passes through the data, are easily eliminated during manual inspections of the microglitch data.**

### 3.4 Significance of the microglitch parameters

The amplitudes of all identified candidate events in  $\nu$  and/or  $\dot{\nu}$  were tested against the null hypothesis that they are mere accumulations of random walks of preferred signs. Following D’Alessandro et al. (1995), Cordes & Downs (1985) the significance test was accomplished by comparing the amplitude of the observed events in  $\nu$  and  $\dot{\nu}$  with the expected standard deviations of idealized large-rate random walk process. **This refers to an accumulation of step functions in pulsar phase residuals and/or its derivatives whose effects, over a time, could mimic genuine discrete rotational discontinuities.** Events are considered real, that is their amplitudes are too large to be due to random walk fluctuations, if  $\Delta\nu \geq \sigma_{\Delta\nu}N$  and  $\Delta\dot{\nu} \geq \sigma_{\Delta\dot{\nu}}N$ : where  $\sigma_{\Delta\nu} = \sqrt{S_1\Delta t}$  and  $\sigma_{\Delta\dot{\nu}} = \sqrt{S_2\Delta t}$  are, respectively, the standard deviations of idealized random walks in  $\nu$  and  $\dot{\nu}$  with strength parameters  $S_1$  and  $S_2$ , respectively,  $N$  is an integer denoting the significance level of the test and  $\Delta t$  is the difference between the arrival times bracketing a candidate event. In this paper,  $\Delta t$  represents the upper bound on the rise time of the microglitch events. For the current sample, values of  $\Delta t$  lie between  $\sim 0.05$  and 40 d, with a mean value of 10 d. Several authors (e.g. CD85, Cordes et al. 1988; DA95) have demonstrated that  $N = 5$  is an appropriate significant level, as it correctly rejects spurious random walk-induced events which could mimic real microglitches. Given the similarity between the HartRAO and JPL pulsar data, in terms of observing frequencies and BTOA signal-to-noise ratio, we equally adopted  $N = 5$  for the current significance test.

Following Chukwude (2002), DA95, CD85, we calculated strength parameters ( $S_1$  and  $S_2$ , respectively) from BTOAs bracketed by any two identified candidate events (hereafter referred to as method A) and from the entire BTOA data available for a pulsar (hereafter referred to as method B). Our presumption is that data sets used in method A, probably, contain no discrete discontinuity and hence has extremely low timing activity. On the other hand, the data set employed in method B incorporates all the rotational discontinuities, including all the microglitches. In principle, methods A and B are expected to yield, respectively, the lower and upper limiting estimates for the strength parameters. The bottom line is that, though the strength parameter estimate is variable in the presence of random walks, its true value should lie within the values obtained from the two methods. Since the rms phase resid-

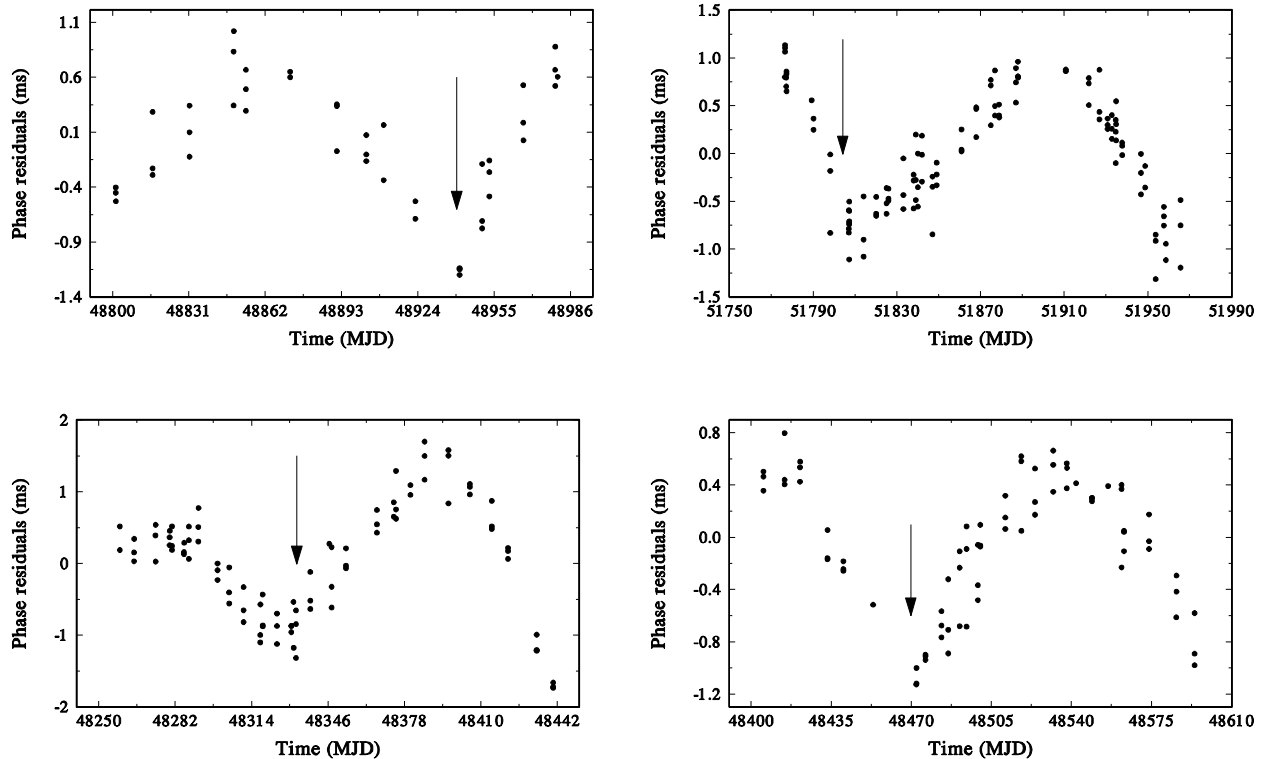


**Figure 3.** The phase residuals around some candidate microglitch events in the pulsar B0740–28, whose observed timing activity show strong evidence for enhanced microglitch activity. The arrows indicate epochs sudden slope changes caused discontinuous rotation

uals of short and long data span lengths are believed to be dominated by events in  $\nu$  and  $\dot{\nu}$ , respectively (DA95; CD85). In view of this fact, we placed greater weight on methods A and B in testing the significance of  $\Delta\nu$  and  $\Delta\dot{\nu}$ , respectively. In addition, the amplitudes of a candidate events were required to exceed the formal standard error by, at least, a factor of two. In principle, the necessary condition that must be satisfied by the jumps in  $\nu$  and  $\dot{\nu}$  is that  $\Delta\nu > 2\epsilon_{\Delta\nu}$  and  $\Delta\dot{\nu} > 2\epsilon_{\Delta\dot{\nu}}$ , respectively, where  $\epsilon_{\Delta\nu}$  and  $\epsilon_{\Delta\dot{\nu}}$  are, the formal standard errors in  $\Delta\nu$  and  $\Delta\dot{\nu}$ , respectively. The formal standard errors were obtained directly from the HartRAO in-house timing analysis routine. We believe that these conditions are stringent enough to filter out most, if not all, spurious events, which could mimic genuine microglitch events.

Over 600 candidate discrete jumps were identified by a combination of the manual and automated search techniques for microglitches. However, only 299 of these events have amplitudes that are large enough to pass the significance tests (and are hereafter referred to as microglitches). The remainder of  $\sim 300$  jumps failed the tests and were consequently rejected, as mere spurious events arising from accumulations of large rate steps of random walks. Out of the 299 microglitches, 266 ( $\sim 90\%$ ) are found to be simultaneously significant in both  $\nu$  and  $\dot{\nu}$  (71 of these were better resolved by the manual search technique). **These represent microglitch events that produced detectable changes in the pulsar spin rate evolution. However, it is believed that several candidate events might have been averaged out in the process leading to the calculation of the  $\Delta\dot{\nu}$  data. Hence, one expects the more objective automatic technique to resolve**

**several more microglitches.** Others are noticeable in either of the spin parameters ( $\nu$  or  $\dot{\nu}$ ). The parameters of the 266 and 33 microglitches are summarized in Tables (1) and (2), respectively. A summary of our results shows that the total microglitches in  $\nu$  and  $\dot{\nu}$  are 285 and 280, respectively. Of the 285 microglitches in  $\nu$ , 148 and 137 of the events have positive and negative amplitudes, respectively, while 139 and 141 of  $\Delta\dot{\nu}$  are, respectively, positive and negative. The fractional jumps in  $\nu$  ( $\Delta\nu/\nu$ ) have minimum and maximum values as  $\sim -8 \times 10^{-9}$  and  $2 \times 10^{-8}$ , respectively, while  $\sim -3 \times 10^{-3}$  and  $4 \times 10^{-3}$  correspond, respectively, to minimum and maximum amplitudes of  $\Delta\dot{\nu}/\dot{\nu}$ . The jumps, nonetheless, show no apparent preferential combination of signs ( $\Delta\nu$ ,  $\Delta\dot{\nu}$ ).

## 4 DISCUSSIONS

### 4.1 Macroglitches among the HartRAO pulsars

Twenty-five of the twenty-six pulsars on routine monitoring at HartRAO are aged more than  $10^5$  years, having an average of  $10^{6.17}$  years. None of the twenty-five has shown any fractional frequency jump larger than  $\sim 10^{-8}$  within the seventeen years of observation. This probably suggests that the interval for large macroglitches in these “middle-aged” (characteristic age  $\sim 10^5 - 10^7$  years) pulsars, if they do occur at all, could be more than the total observation span of  $\sim 425$  years.

The only one in the sample that has shown a large jump, PSR 1727–47, is younger than  $10^5$  years. Within this period, the pulsar had two large macroglitches of amplitudes

**Table 1.** Parameters of the microglitches, whose amplitudes are simultaneously significant in both  $\nu$  and  $\dot{\nu}$ , for the 20 HartRAO radio pulsars observed using both the manual and automatic search techniques.

Pulsars (PSR B) (1)	Epoch (MJD) (2)	$\Delta\nu/\nu$ ( $10^{-9}$ ) (3)	ERR <sup>a</sup> (4)	$\Delta\dot{\nu}/\dot{\nu}$ ( $10^{-3}$ ) (5)	ERR <sup>a</sup> (6)	Pulsars (PSR B) (1)	Epoch (MJD) (2)	$\Delta\nu/\nu$ ( $10^{-9}$ ) (3)	ERR <sup>a</sup> (4)	$\Delta\dot{\nu}/\dot{\nu}$ ( $10^{-3}$ ) (5)	ERR <sup>a</sup> (6)	
0736–40	47076	0.43	3	−0.15	2	0835–41	46271	−0.43	5	2.2	4	
	47751	0.12	2	−0.16	2		47207	0.07	1	0.11	1	
	47943 <sup>+</sup>	0.25	3	0.17	2		47840	0.12	1	−0.079	3	
	48283	0.13	2	0.75	2		49780	−0.13	6	−0.064	3	
	48502	1.08	8	−0.89	4		0959–54	46479	6	2	−1.8	5
	49292 <sup>+</sup>	0.34	4	0.83	6			47477 <sup>+</sup>	2.2	2	0.32	6
	50395 <sup>+</sup>	−0.67	2	−0.44	2			48138 <sup>+</sup>	2.4	4	−0.64	2
	50612	0.17	2	0.42	1			48490	−1.64	8	−0.46	2
	51997	0.13	2	−0.83	3			48600	0.8	2	0.75	9
	52224	0.45	6	0.55	8			49241 <sup>+</sup>	−1.79	8	0.80	6
0740–28	52409 <sup>+</sup>	−0.86	5	−1.2	4	50845 <sup>+</sup>	1.74	8	1.19	4		
	46653 <sup>+</sup>	0.46	7	−0.052	5	52236 <sup>+</sup>	−3.7	1	1.98	9		
	46806	1.2	4	−0.08	2	1054–62	47153	0.37	8	−0.28	5	
	46992	−0.17	6	0.057	6		47913	0.35	5	0.19	3	
	47085	−0.06	1	−0.026	5		48190 <sup>+</sup>	−0.95	8	0.26	6	
	47358 <sup>+</sup>	0.72	3	−1.05	9		48301	0.69	6	0.18	3	
	47450	0.39	5	−0.146	7		48480 <sup>+</sup>	1.5	2	−0.56	3	
	47576	−0.38	8	−0.08	2		49169	0.12	4	0.06	2	
	47681 <sup>+</sup>	2.75	8	−1.6	2		49378	0.29	8	−0.19	6	
	47736	−0.55	9	0.09	2		49631	0.18	5	−0.09	2	
	47843	−0.75	5	−0.10	1		50025	−0.5	2	0.12	3	
	47956	−0.95	6	0.070	5		50386	0.20	5	0.47	2	
	48084	−0.62	7	0.034	6	50782 <sup>+</sup>	3.2	4	−0.88	8		
	48246 <sup>+</sup>	−2.3	3	−0.99	2	50997 <sup>+</sup>	2.3	4	−0.59	5		
	48345	1.4	2	2.5	4	52008	−0.12	3	0.12	3		
	48427	−0.7	2	−0.29	4	52166	−0.75	9	−0.11	5		
	48470 <sup>+</sup>	−2.4	2	2.6	2	1221–63	48147	−0.06	1	−0.022	1	
	48646	1.14	9	−0.07	1		48788 <sup>+</sup>	0.87	4	0.79	7	
	48852 <sup>+</sup>	1.23	8	0.25	2		49308	0.06	2	0.05	1	
	48940	1.2	2	0.6	2		49814 <sup>+</sup>	1.5	4	−0.19	6	
	49050	2.8	3	1.55	3		50830	−0.17	4	0.04	1	
	49287	2.0	2	0.96	3		50960 <sup>+</sup>	3.6	5	0.96	9	
	49353 <sup>+</sup>	−2.2	5	0.35	2	51931	1.2	3	−0.9	3		
	49621	−0.16	4	−0.092	4	1240–64	47460	0.18	2	−0.12	3	
	49915	0.89	4	0.070	3		47960 <sup>+</sup>	−0.33	4	0.09	2	
	50008	−0.5	2	0.16	2		48464	0.19	2	0.12	3	
	50185	0.65	8	−1.3	2		49030	−0.033	2	0.29	2	
	50376 <sup>+</sup>	1.19	9	−0.9	2		49610	0.32	3	−0.13	1	
	50529	0.77	8	−0.08	1		50092	−0.68	5	0.18	2	
	50609	0.4	1	−0.18	2		50503 <sup>+</sup>	−0.78	6	−0.59	9	
50782	1.3	2	1.0	2	50677		−0.11	3	0.014	2		
50978 <sup>+</sup>	1.45	8	0.69	3	51871		−0.09	2	−0.06	1		
51109	1.5	2	−0.53	3	1323–58		47586 <sup>+</sup>	1.43	8	1.5	3	
51785 <sup>+</sup>	−1.93	8	0.96	2		47878	−0.16	2	1.30	2		
51880	−0.93	8	0.38	2		47955 <sup>+</sup>	−1.45	5	1.07	8		
51970	−0.19	7	−0.22	1		48212	−1.03	4	0.85	2		
52030 <sup>+</sup>	2.32	9	−1.38	9		48700	−0.69	2	−1.28	1		
52111	−0.7	2	−0.11	3		49245	−0.78	5	0.43	2		
52249	−1.2	2	0.08	2		49792	−1.82	7	−0.82	3		
52370 <sup>+</sup>	−0.28	5	0.25	2		49879	0.47	4	0.28	2		

<sup>a</sup> The formal standard error and refers to the least significant digit

<sup>+</sup> Indicates epochs of events whose jump parameters were better resolved by the manual technique

**Table 1** – *continued*

Pulsars (PSR B) (1)	Epoch (MJD) (2)	$\Delta\nu/\nu$ ( $10^{-9}$ ) (3)	ERR <sup>a</sup> (4)	$\Delta\dot{\nu}/\dot{\nu}$ ( $10^{-3}$ ) (5)	ERR <sup>a</sup> (6)	Pulsars (PSR B) (1)	Epoch (MJD) (2)	$\Delta\nu/\nu$ ( $10^{-9}$ ) (3)	ERR <sup>a</sup> (4)	$\Delta\dot{\nu}/\dot{\nu}$ ( $10^{-3}$ ) (5)	ERR <sup>a</sup> (6)
	50150 <sup>+</sup>	0.99	9	1.23	9		47860	1.5	4	-1.9	5
	50455	-0.92	6	0.98	3		48000	1.1	3	-1.2	3
	50670 <sup>+</sup>	-0.55	8	-0.58	8		48316	-0.99	9	-0.32	2
	50964	0.48	8	-0.64	5		48548	0.75	6	0.54	5
	51020	0.5	1	-0.56	5		49085 <sup>+</sup>	-1.9	2	-2.46	1
	51880	1.08	7	-0.66	4		49206	0.60	3	1.78	9
1323-62	52338	-1.5	3	-1.2	4		50210	-1.5	2	-0.57	3
	46769	-0.7	2	0.06	2		50673 <sup>+</sup>	-1.7	8	-2.58	6
	46940	-1.92	10	-0.75	1		52276	1.6	2	1.52	10
	47163	-1.4	3	0.28	4	1449-64	48360	0.22	1	0.042	6
	47666 <sup>+</sup>	0.82	6	-0.17	1		50212	0.05	1	0.014	4
	47729 <sup>+</sup>	-0.90	5	0.8	2		50768	0.12	5	0.05	2
	47875	3.8	8	0.6	2		50835	-0.08	3	-0.06	1
	48059	0.40	7	-0.19	4	1556-44	48861	-0.06	1	0.008	3
	48242 <sup>+</sup>	-1.3	4	0.8	2		50104	0.08	1	-0.05	1
	48371	-0.63	8	0.32	3		51166	0.15	5	-0.08	1
	48459 <sup>+</sup>	0.67	9	0.48	5	1557-50	47413	-0.12	2	-0.035	5
	48670	-0.56	6	-0.9	2		47913	-0.04	1	0.0130	2
	48860 <sup>+</sup>	0.69	9	0.65	4		47960	-0.18	2	-0.025	4
	48939	-1.4	2	0.55	4		48392 <sup>+</sup>	-0.66	5	-0.095	3
	49150 <sup>+</sup>	1.6	2	0.19	3		48524	0.12	2	0.058	4
	49334	-1.5	3	-0.38	4		48552	-0.18	4	-0.083	6
	49408	-0.62	8	-0.44	3		48928 <sup>+</sup>	0.74	3	-0.19	4
	49581	0.9	2	0.16	4		49326	-0.12	2	0.06	1
	49812	0.42	8	-0.26	2		49750 <sup>+</sup>	-0.28	3	0.092	5
	49906	-0.36	5	0.07	2		50018	-0.06	1	0.10	1
	50019	1.3	2	0.18	3		50764 <sup>+</sup>	-0.52	2	0.076	5
	50104	-0.9	2	-0.20	4		51274	-0.32	5	-0.07	2
	50255 <sup>+</sup>	-1.27	9	-0.38	5		52007	-0.09	3	0.06	2
	50351	2.2	3	-0.64	9	1642-03	47156	2.15	7	1.93	4
	50414	-1.07	9	0.23	4		47740	0.45	3	-1.28	3
	50646	-2.6	3	-0.88	6		48164 <sup>+</sup>	-2.81	3	1.79	6
	50824	-1.3	3	0.41	8		48939	0.33	2	-0.51	1
	50970 <sup>+</sup>	4.5	8	1.7	5		49358	1.16	9	0.70	6
	51167	1.6	2	-0.24	8		49646	-0.42	2	-0.85	2
	51950	-1.8	4	-0.5	1		50280	-0.59	3	1.24	3
	52073	-2.1	4	0.39	6		50650 <sup>+</sup>	1.9	2	1.48	10
1356-60	52264 <sup>+</sup>	1.9	2	0.67	4		50978	-0.22	3	-1.59	2
	47855	0.21	4	-0.12	1		51173	-0.8	2	-1.3	2
	48680	-1.9	5	-0.9	2		52183 <sup>+</sup>	-1.85	8	1.72	2
	48847	0.45	7	-0.033	8	1706-16	48131 <sup>+</sup>	-3.5	8	2.7	5
	49388	0.38	6	-0.06	2		48535	-0.89	9	-1.7	4
	49685	0.65	4	0.047	3		48615	0.56	5	3.3	3
	49713	-0.53	8	-0.04	1		49101 <sup>+</sup>	-3.6	5	-3.5	6
	50101 <sup>+</sup>	-1.68	9	-0.85	1		49257	1.15	8	-0.65	3
	50356	0.022	4	0.049	8		50541	1.0	2	0.31	5
	50757	0.26	6	-0.056	6		51002	0.30	6	-0.22	1
	51150	0.8	2	0.85	3		51830	-0.48	4	-0.36	6
1358-63	52009	-0.12	4	-0.07	1	1727-47	46383	-1.5	5	0.06	2
	47725 <sup>+</sup>	-1.8	3	-2.38	9		46913	-1.2	4	0.034	8

<sup>a</sup> The formal standard error and refers to the least significant digit<sup>+</sup> Indicates epochs of events whose jump parameters were better resolved by the manual technique



Table 1 – continued

Pulsars (PSR B) (1)	Epoch (MJD) (2)	$\Delta\nu/\nu$ ( $10^{-9}$ ) (3)	ERR <sup>a</sup> (4)	$\Delta\dot{\nu}/\dot{\nu}$ ( $10^{-3}$ ) (5)	ERR <sup>a</sup> (6)	Pulsars (PSR B) (1)	Epoch (MJD) (2)	$\Delta\nu/\nu$ ( $10^{-9}$ ) (3)	ERR <sup>a</sup> (4)	$\Delta\dot{\nu}/\dot{\nu}$ ( $10^{-3}$ ) (5)	ERR <sup>a</sup> (6)
	47123	0.5	1	-0.017	2		46979	0.92	9	0.42	8
	47260 <sup>+</sup>	9.3	3	-1.95	6		47132	1.2	6	-0.48	9
	47499	-0.33	4	-0.07	2		47322 <sup>+</sup>	3.5	6	0.75	8
	47889	0.6	2	0.50	5		47764	2.4	7	0.3	1
	48540	-0.26	8	0.08	1		48140 <sup>+</sup>	1.9	5	0.25	5
	49200 <sup>+</sup>	13.6	8	-2.54	2		48210	-2.07	8	0.5	2
	49817	0.84	7	-0.12	1		48451	0.6	2	0.08	2
	50088	-1.13	6	-1.04	2		48580	-7.8	2	-0.89	9
	50388	0.97	7	0.033	1		48747	-0.9	4	-0.16	4
	50662	1.3	3	0.38	8		49132	-1.7	6	-0.7	3
	52108	0.7	2	0.05	1		49279	-4.7	9	0.6	2
	52300	3.76	8	-0.58	6		49876	3.6	2	-0.38	2
1749–28	46805	-0.50	4	0.12	1		50150 <sup>+</sup>	4.9	3	-2.35	7
	46990 <sup>+</sup>	5.03	7	-1.6	2		50495	-1.2	2	0.18	6
	47315	0.58	2	0.23	2		50585	-0.8	2	-0.28	3
	47660	-0.31	2	-0.13	1		50997	-0.98	4	-0.68	9
	48098 <sup>+</sup>	3.5	8	0.79	3		51905 <sup>+</sup>	32	3	1.68	8
	48485	0.48	6	-0.42	4		52041	-0.83	4	-0.74	9
	48701 <sup>+</sup>	-1.3	2	0.89	6		52110	0.8	3	1.92	8
	48806	-0.96	6	0.36	5		52273	12.6	6	-2.22	5
	48916 <sup>+</sup>	2.3	5	0.62	9	1929+10	47391	-0.027	6	-0.067	8
	49173	-0.32	6	-0.18	5		47670 <sup>+</sup>	-0.62	4	-0.21	8
	49756 <sup>+</sup>	0.8	2	-0.6	1		48360 <sup>+</sup>	0.74	7	-0.39	2
	49964	0.30	5	0.57	3		48446	-0.28	2	0.06	1
	50260	1.09	6	0.41	3		49064	-0.23	4	-0.16	2
	50356	-0.33	5	-0.39	4		49205	-0.27	5	0.15	2
	50408 <sup>+</sup>	0.56	6	-1.12	8		49542	-0.16	5	0.18	3
	50583	-0.31	6	0.13	4		49710	-0.013	2	-0.012	2
	50727	0.68	9	-0.15	2		50182	-0.05	1	0.33	4
	51108 <sup>+</sup>	1.2	2	-0.65	7		50266	-0.07	2	-0.38	3
	51250	0.65	6	-0.21	1		50773	0.09	2	0.14	2
	52075 <sup>+</sup>	-0.76	4	0.19	1		51198	0.19	3	0.10	2
1822–09	46838	-2.2	5	-0.17	6		52081	0.5	1	-0.25	3

<sup>a</sup> The formal standard error and refers to the least significant digit

<sup>+</sup> Indicates epochs of events whose jump parameters were better resolved by the manual technique.

$\Delta\nu/\nu = 1.37 \times 10^{-7}$  and  $1.25 \times 10^{-7}$  at MJD 49382 and 52476, respectively. There was also a smaller one, though larger than the jumps reported here, at MJD 50718 with  $\Delta\nu/\nu = 3.2 \times 10^{-8}$ . Very many other microglitches have been reported in this paper for this pulsar.

This is in agreement with earlier suggestions that the oldest pulsars, like the millisecond pulsars are free from macroglitches. In a statistical study of 48 macroglitches from 18 pulsars, Lyne et al. (2000) found that the glitch activity decreases linearly with decreasing rate of slowdown. Also, Urama & Okeke (1999) reported that smaller values of  $\Delta\nu/\nu$  and  $\Delta\dot{\nu}/\dot{\nu}$  are seen to be more common in pulsars older than  $10^5$  years and that no glitch has been observed in conventional radio pulsars older than  $10^7$  years.

## 4.2 Microglitches and timing noise events

The observed timing activity of 20 pulsars are found to be at levels (with  $\sigma_R/\sigma_W > 5$ ) considered significant for meaningful microglitch analyses. For the remainder of 6 pulsars, the observed timing activity over  $\sim 13$  yr period is almost indistinguishable from measurement uncertainty. The intrinsic scatter in the BTOAs of these objects have amplitudes in excess of 20 ms (see Chukwude 2007) which could easily and effectively swamp any low level timing activity in the pulsars. This anomalously large scatter in the data could be attributed to HartRAO local observing system parameters: high observing frequencies (13 and 18 cm) and the narrow receiver band of 10 MHz. These parameters could combine to further reduce the precision of measurements of the pulse times of arrival. This would ultimately degrade the BTOAs of pulsars which intrinsically exhibit low level of timing activity. Another possibility is that some of the pulsars are intrinsically faint objects. For instance, previous indepen-

**Table 2.** Parameters of the 33 microglitches, whose amplitudes are significant in only  $\nu$  or  $\dot{\nu}$ , observed using the automated search technique

Pulsars (PSR B) (1)	Epoch (MJD) (2)	$\Delta\nu/\nu$ ( $10^{-9}$ ) (3)	ERR <sup>a</sup> (4)	$\Delta\dot{\nu}/\dot{\nu}$ ( $10^{-3}$ ) (5)	ERR <sup>a</sup> (6)	Pulsars (PSR B) (1)	Epoch (MJD) (2)	$\Delta\nu/\nu$ ( $10^{-9}$ ) (3)	ERR <sup>a</sup> (4)	$\Delta\dot{\nu}/\dot{\nu}$ ( $10^{-3}$ ) (5)	ERR <sup>a</sup> (6)
0835–41	47437	–	–	–0.099	3		50607	–1.53	5	–	–
	50961	–0.25	1	–	–	1240–64	47423	0.26	2	–	–
	51201	–0.36	3	–	–		48712	–	–	–0.18	5
0959–54	47570	–0.95	4	–	–		49076	–	–	–0.65	2
	47983	–2.37	4	–	–	1323–62	49688	–	–	0.18	3
	48017	1.55	5	–	–	1358–63	49733	–	–	–0.47	2
	49076	–	–	–0.65	2		48555	–	–	0.69	3
	49511	–1.8	3	–	–		49767	–	–	0.49	6
	50032	1.82	6	–	–		50251	–	–	–0.69	8
	50455	1.29	4	–	–	1557–50	47599	1.29	9	–	–
	49711	–	–	0.25	6		49006	–0.29	6	–	–
	50696	–	–	0.5	1	1749–28	50395	–	–	0.79	5
	50983	0.85	3	–	–	1822–09	47960	–	–	0.12	2
	51899	3.85	5	–	–		48797	–	–	–0.039	6
	52210	–2.2	2	–	–		50098	–5.7	7	–	–
1706–16	49880	–0.86	8	–	–		51908	–2.5	3	–	–
1727–47	48886	0.35	5	–	–						

<sup>a</sup> The formal standard error and refers to the least significant digit

dent analyses of, presumably, higher precision, timing data on some of these pulsars (1133+16, 1426–66, 1451–68 and 2045–16) do not reveal any appreciable level of timing activity (DA95; CD85).

For the sub-sample of 20 pulsars extensively used in current analyses, the results are both phenomenal and unprecedented in the history of microglitch observations in radio pulsars. The automatic technique identified a total of 266 jumps that are simultaneously significant in both pulsar rotation frequency and spin-down rate. Only 71 (or < 30%) of these microglitches were equally resolved by the traditional manual method. In addition, the automated technique observed 19 and 14 significant jumps in only  $\nu$  and  $\dot{\nu}$ , respectively. The fractional jumps in  $\nu$  and  $\dot{\nu}$  ( $\Delta\nu/\nu$  and  $\Delta\dot{\nu}/\dot{\nu}$ , respectively) have all possible combinations of signs. For the 266 microglitch events, we found  $(\Delta\nu/\nu, \Delta\dot{\nu}/\dot{\nu}) = (+, +), (+, -), (-, -)$  and  $(-, +)$  as the signatures of 69, 68, 66 and 63 events, respectively. It is worthy of note that the distribution of these events is not statistically different from random. Our results also reveal large dispersions,  $\sim 4$  orders of magnitude, in observed sizes of the jumps in both spin parameters. Strikingly, the observed fractional jumps in  $\nu$  and  $\dot{\nu}$  have sizes whose magnitudes are in the range of  $\sim 2 \times 10^{-11} - 2 \times 10^{-8}$  and  $5 \times 10^{-6} - 4 \times 10^{-3}$ , respectively. Typical median values for  $|\Delta\nu/\nu|$  and  $|\Delta\dot{\nu}/\dot{\nu}|$  are  $\sim 0.8 \times 10^{-9}$  and  $0.4 \times 10^{-2}$ , respectively.

Arguably, we have presented what is as yet the most in-depth and successful observations of microglitch phenomenon in slow radio pulsars. Nonetheless, there had been some attempts in the past to observe these small amplitude discrete events in pulsar rotation rates. Cordes & Downs (1985) carried out extensive analyses of the BTOAs of 17 pulsars obtained at Jet Propulsion Laboratory (JPL) between 1968 and 1982. In the framework of the manual tech-

nique, the authors identified a total of 74 candidate events in  $P$  and  $\dot{P}$ . However, only 43 of these events were found to be significant – 10 simultaneously in  $P$  and  $\dot{P}$ , while 17 and 16 were separately significant in  $P$  and  $\dot{P}$ , respectively. Similar analysis, based on a sample of 26 pulsars observed at Mt. Pleasant Observatory between 1987 and 1991 (D’Alessandro et al. 1995) yielded about 35 significant microjump events from about 70 candidate events. A breakdown of the events shows that while 5 events were noticeable in both  $\nu$  and  $\dot{\nu}$ , 20 and 10 were significant only in  $\nu$  and  $\dot{\nu}$ , respectively. In comparison, current analyses identified  $\sim 300$  microjumps from just 20 pulsars, which is about a factor of 4 in excess of all the hitherto known radio pulsar microglitches.

As a check on the reliability of the methods and the reality of the results, it might be necessary to compare it with those of previous studies. It is noteworthy that the HartRAO and Tasmanian timing data on 16 pulsars overlap each other, up to 1991. Remarkably, over 90% of the microglitch events reported for these objects by DA95 also show up in current analyses and the results (epochs and signatures of the events) are generally in good agreements. However, in terms of the jump sizes, our results differ considerably with those published by DA95, nonetheless they are still of the same order of magnitude. Irrespective of sign, we find that the amplitudes of the current microjumps are, in most cases, considerably larger than those reported by DA95, suggesting a better resolution of the microevents. This is particularly true for  $\Delta\dot{\nu}$ , where our measurements could be up to a factor of 4 larger than those observed by DA95. As a consequence, most of the candidate microglitch events found to be insignificant in DA95 were observed to be significant in current analysis.

The unprecedented improvements in both the number and amplitudes of pulsar microglitches could be attributed

to some unique features of the current timing data: long time coverage ( $\sim 16$  yrs) and shorter sampling intervals. Shorter data sampling intervals would naturally lead to better time resolutions of events. Expectedly, this would reduce the uncertainty in event epoch, resulting in significantly improved estimates of jump sizes. Glitch analyses (e.g. Flanagan 1990) have demonstrated how the resolution of jump parameters strongly depended on the accuracy of the epochs of the events. The rise times of the events ( $\Delta t$ ) for current analysis lie between 0.05 and 40 d, with a median value of  $\sim 10$  d. This implies that the epochs of the microglitches reported in this paper are improved by a factor of, at least, 4 over those of JPL and Tasmanian data sets, where  $\Delta t$  are in the range of  $\sim 6 - 154$  d and  $13 - 255$  d, respectively. This could, almost certainly, lead to better resolution of event sizes. It is noteworthy that our techniques identified most of the small macroglitches reported previously from independent analyses timing data on the pulsars B0740–28 and B1240–64 (Janssen & Stappers 2006; D’Alessandro & McCulloch 1997). Again, our results on the jump parameters (epochs, amplitudes and signatures) are remarkably in good agreement with previous results. However, current methods were able to identify almost all the jumps in  $\dot{\nu}$ , which previous analyses could not resolve owing to large uncertainties in event epochs. Hence, the seemingly high sensitivity of the current analysis could be attributed to the dramatic improvement in precision of the events’ epochs in HartRAO data set.

A key challenge in microglitch observation analyses has remained the extraordinary difficulty in distinguishing between real and spurious events. Cordes & Downs (1985) suggested that microjumps could be identified by demonstrating that they are too large to be mere fluctuations produced by accumulation of many, much smaller events of random walk origin. Previous studies (DA95; Cordes et al. 1988; CD85) have relied largely on the significance tests, using timing noise strength parameters, to isolate significant events. However, Cordes & Downs (1985) have highlighted the strong dependence of the current method of testing the significance of microglitch events on the rise time of the event  $\Delta t$ . For instance, the standard deviations could possibly be over-estimated or under-estimated for very small or very large  $\Delta t$ , respectively. This could cause leakage of spurious events with large amplitudes or rejection of extremely small-amplitude discrete events. The former scenario might be the case in previous analyses (DA95; CD85), while current data appear to favour the later scenario. With a median event rise time ( $\Delta t$ ) of  $\sim 10$  d, it is feared that both  $\sigma_{\Delta\nu}$  and  $\sigma_{\Delta\dot{\nu}}$  could have been significantly under-estimated in some cases, causing significant leakage of spurious events into the sample of real discrete events (e.g. Chukwude 2002). However, we are optimistic that the  $2\text{-}\sigma$  standard formal error condition imposed on the size identified microglitches is stringent enough to filter out all or, at least, most spurious events.

## 5 SUMMARY

The phenomenon of microglitches in slow radio pulsars have been probed deeply using the manual and automatic search techniques. An extensive analysis of a sub-sample of 20 pulsars, whose timing data span  $\sim 16$  yrs in time and have a

median sampling frequency of  $\sim 0.1 \text{ d}^{-1}$ , yielded a phenomenal 299 microglitch events in pulse rotation frequency and its first derivative. This translates to more than a factor of 3 increase in the statistics of the observed microglitch events. The jumps show no preferred signs and have amplitudes that span about 3 orders of magnitude in both parameters, irrespective of signs. Current results have, among other things, demonstrated the prevalence of microglitch phenomenon in slow radio pulsars.

## ACKNOWLEDGMENTS

This work was done, in part, when AEC was visiting the Abdus Salam International Centre for Theoretical Physics, Trieste, Italy as a Junior Associate. He is grateful to the Swedish International Development Agency (SIDA) for supporting his visit to ICTP with a travel grant. The authors wish to acknowledge the Director of HartRAO and Dr. C. S. Flanagan for giving them access to the Observatory pulsar data.

## REFERENCES

- Alpar, M. A., Anderson, P. W., Pines, D., Shaham, J., 1984, *ApJ*, 278, 533
- Alpra, M. A., Chau, H. F., Cheng, K. S., Pines, D. 1996, *ApJ*, 459, 706
- Arons, J., in *IAU Symposium 95, Pulsars*, ed. W. Sieber and R. Wielebinski (Dordrecht: Reidel), 69
- Bevington, P. R., 1969, *Data Reduction and Error Analysis for Physical Sciences* (McGraw-Hill Book Company)
- Chukwude, A. E., 2002, Ph.D. Thesis, University of Nigeria, Nsukka
- Chukwude, A. E., 2007, *Chin. J. Astron. Astrophys.* 7, 521
- Cordes, J. M., Greenstein, G., 1981, *ApJ*, 245, 1060
- Cordes, J. M., Helfand, D. J., 1980, *ApJ*, 239, 640
- Cordes, J. M., Downs, G. S., 1985, *ApJS*, 59, 343
- Cordes, J. M., Downs, G. S., Krause-Polstorff, J., 1988, *ApJ*, 330, 847
- D’Alessandro, F., 1997, *Ap&SS*, 246, 73
- D’Alessandro, F., McCulloch, P. M., 1997, *MNRAS*, 292, 879
- D’Alessandro, F., McCulloch, P. M., Hamilton, P. A., Deshpande, A. A., 1995, *MNRAS*, 277, 1046
- Flanagan, C. S., 1995, PhD thesis, Rhodes University, Grahamstown, South Africa
- Flanagan, C. S., 1990, *Nat*, 345, 416
- Goldreich, P., Julian, W. H., 1969, *ApJ*, 157, 869
- Glampedakis, K., & Andersson, N., 2009, *PhRvL*, 102, 1101
- Hobbs, G. B., Edwards, R. T., Manchester, R. N., 2006, *MNRAS*, 369, 655
- Janssen, G. H., Stappers, B. W., 2006, *A&A*, 457, 611
- Link, B., Epstein, R., Baym, G., 1993, 1993, *ApJ*, 403, 285
- Lorimer, D. & Kramer, M. 2005, *Handbook of Pulsar Astronomy* (Cambridge University Press)
- Lyne, A. G., 1987, *Nat*, 326, 569
- Lyne, A. G., Pritchard, R. S., 1987, *MNRAS*, 229, 223
- Lyne, A. G., Graham-Smith, F., 1998, *Pulsar Astronomy* (Cambridge University Press)

- Lyne, A. G., Pritchard, R. S., Kaspi, V. M., Bailes, M., Manchester, R. N., Taylor, H., Arzoumanian, Z., 1996, *MNRAS*, 281, 14
- Lyne, A. G., Shemar, S. L., Smith, F. G., 2000, *MNRAS*, 315, 534
- Manchester, R. N., Taylor, J. H., 1977, *Pulsars* (San Francisco: Freeman)
- Melatos, A., Peralta, C., 2007, *ApJ*, 662, 99
- Melatos, A., Peralta, C., Wytke, S. B., 2008, *ApJ*, 672, 1103
- Melatos, A., Warszawski, L., 2009, *ApJ*, 700, 1524
- Middleditch, J., Marshall, F. E., Wang, Q. D., Gotthelf, E. V., Zhang, W., 2006, *ApJ*, 652, 1531
- Pacini, F., *Nature*, 219, 145
- Peralta, C., Melatos, A., Giacobello, M., Ooi, A., 2006, *ApJ*, 651, 1079
- Ruderman, M., Zhu, T., Chen, K., 1998, *ApJ*, 492, 267
- Urama, J. O., 2002, *MNRAS*, 330, 58
- Urama, J. O., Okeke, P. N., 1999, *MNRAS*, 310, 313
- Wang, N., Wu, X., Manchester, R. N., Zhang, J., Lyne, A. G., Yusup, A., 2001, *Chin. J. Astron. Astrophys.*, 1, 195
- Warszawski, L., Melatos, A., 2008, *MNRAS*, 390, 175

This paper has been typeset from a  $\text{\TeX}/\text{\LaTeX}$  file prepared by the author.